Supplementary Materials: Setting plasma immersion ion implantation of Ar^+ parameters towards electroforming-free and self-compliance HfO_2-based memristive structures

Olga Permiakova *, Sergey Pankratov, Alexandr Isaev, Andrew Miakonkikh, Yuri Chesnokov, Andrey Lomov and Alexander Rogozhin *
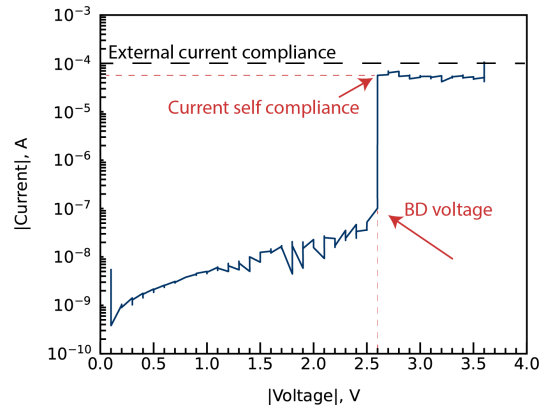
Figure S1. Example of electroforming process of $Pt/HfO_2/HfO_XN_Y/TaN$ after plasma immersion ion implantation of Ar^+ with energy 2 keV and fluence $7.0 \cdot 10^{15}\,cm^{-2}$.
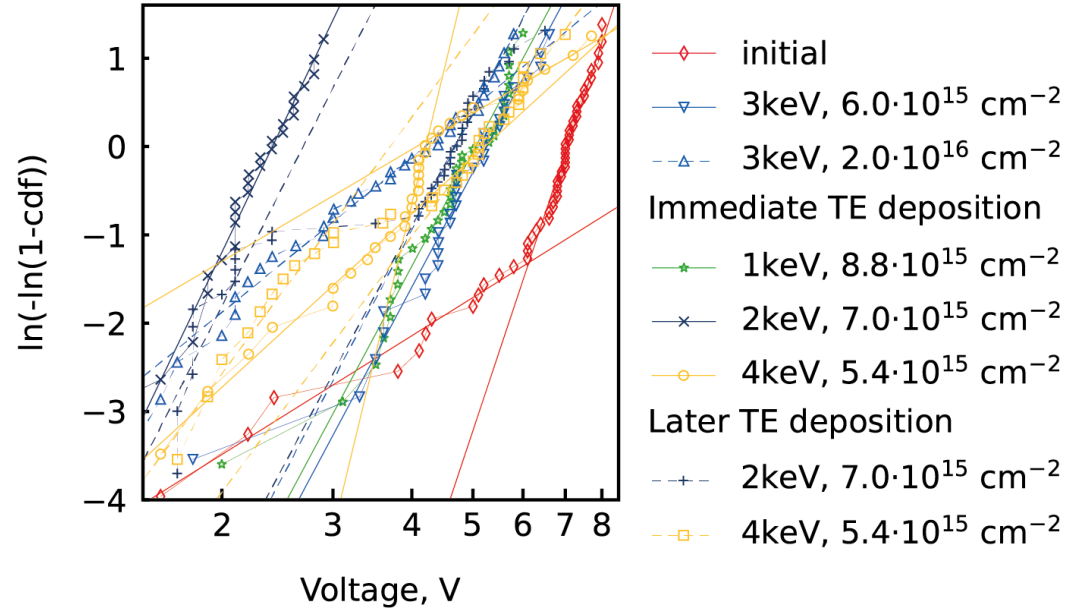

Figure S2. Fitted Weibull distributions of breakdown voltages for $Pt/HfO_2/HfO_XN_Y/TaN$ structures subjected to plasma immersion ion implantation of Ar^+.
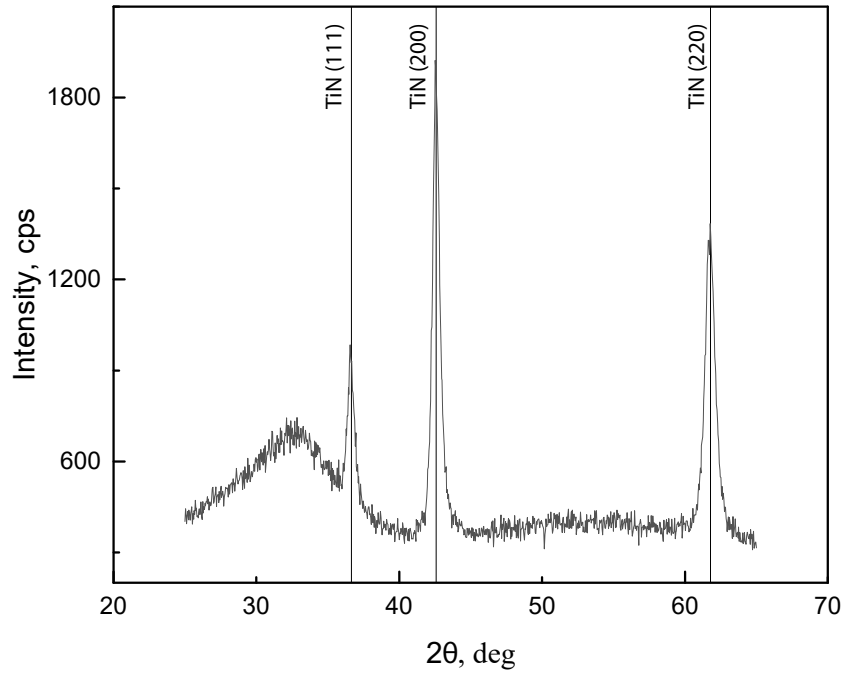
Figure S3. GIXRD spectra of the $HfO_2/HfO_XN_Y/TaN$ structure without implantation.

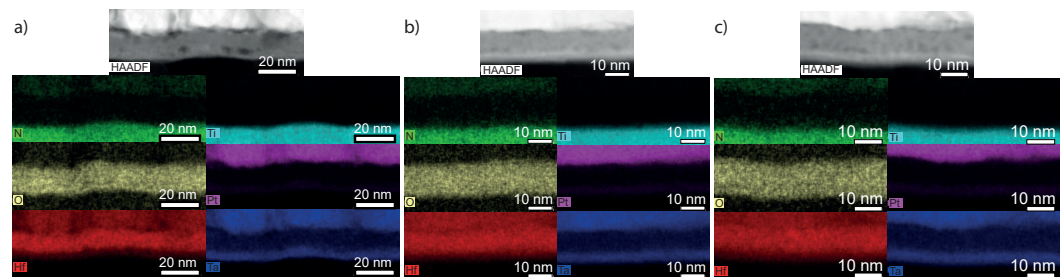**Figure S4.** Cross-sectional HAADF-STEM image of the $Pt/HfO_2/HfO_XN_Y/Ta$ structures and corresponding EDS mapping of N, Ti, O, Pt, Hf and Ta without deconvolution. a) Cross-sectional HAADF-STEM image of the reference structure. b) Cross-sectional HAADF-STEM image of the structure after Ar^+ plasma immersion ion implantation with the energy of 2 keV and fluence of $7.0 \cdot 10^{15}$ cm^{-2}. c) Cross-sectional HAADF-STEM image of the structure after Ar^+ plasma immersion ion implantation with the energy of 4 keV and fluence of $5.4 \cdot 10^{15}$ cm^{-2}

c) 3 keV, 2.0·10^{16} cm^{-2}

b) 3 keV, 6.0·10^{15} cm^{-2}

e) 2 keV, 7.0·10^{15} cm^{-2}

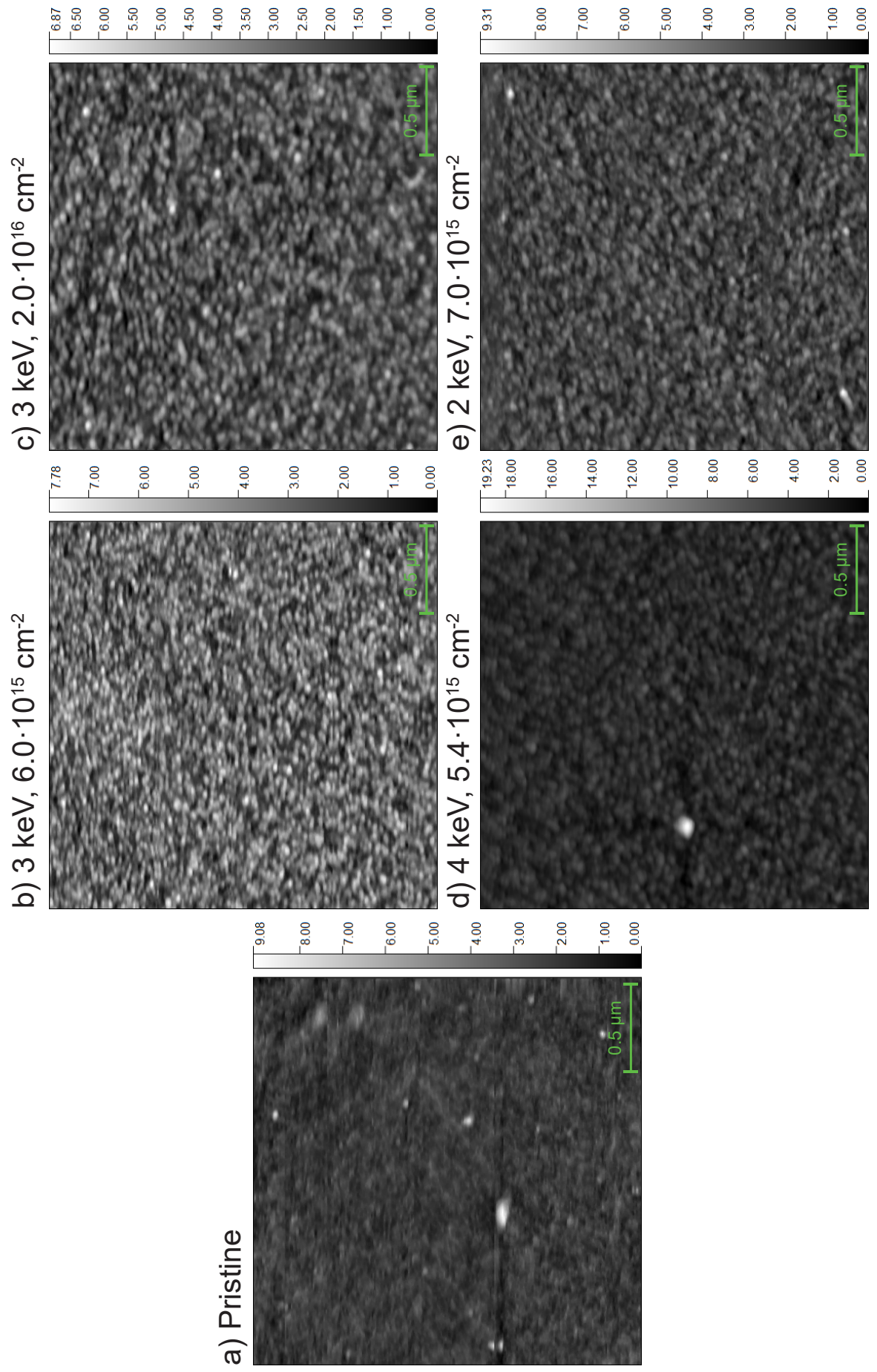d) 4 keV, 5.4·10^{15} cm^{-2}

a) Pristine

Figure S5. Images used to estimate surface roughness measured via AFM. The images were processed with a Fourier filter.
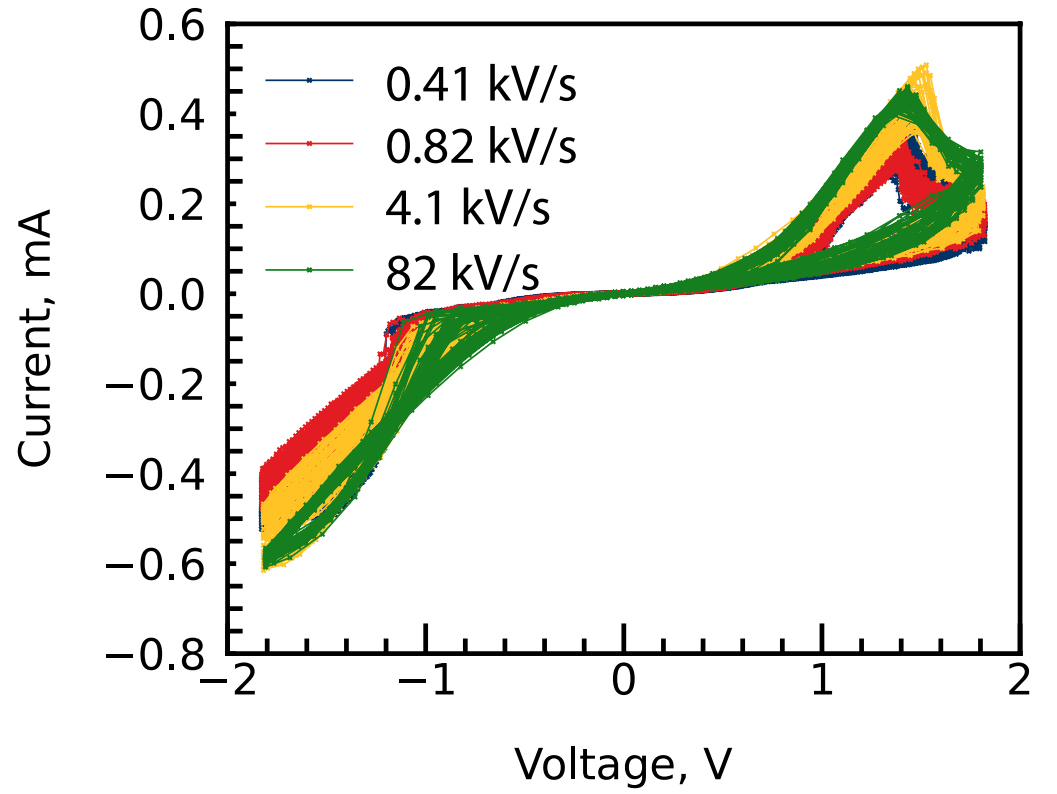
Figure S6. I-V characteristics of Pt/HfO$_2$/HfO$_X$N$_Y$/TaN structures subjected to plasma immersion ion implantation of Ar$^+$ with energy of 2 keV and fluence of $7 \cdot 10^{15}$ cm^{-2}.
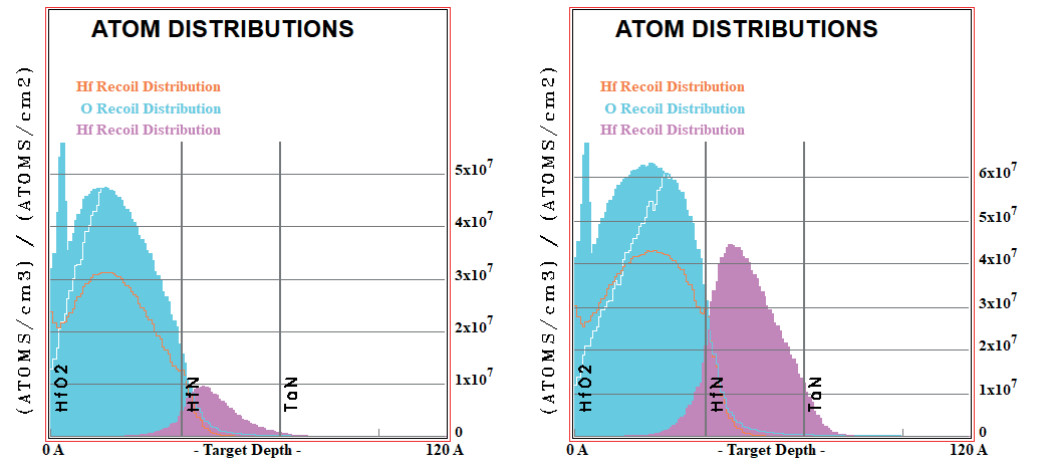

Figure S7. SRIM simulation of Hf atom displacements induced by Ar$^+$ plasma immersion ion implantation in HfO$_2$/HfO$_X$N$_Y$/TaN structure with energies of 2 keV (a) and of 4 keV (b).